Urban Climate 55 (2024) 101936

Contents lists available at ScienceDirect

Urban Climate

journal homepage: www.elsevier.com/locate/uclim

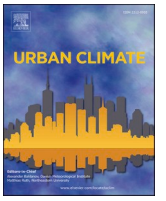

How virtuous are the bias corrected CMIP6 models in the simulation of heatwave over different meteorological subdivisions of India?

Saumya Singh [a], R.K. Mall [a,*], Praveen K. Singh [a], R. Bhatla [a,b], Pawan K. Chaubey [a]

[a] DST-Mahamana Centre of Excellence in Climate Change Research, Institute of Environment and Sustainable Development, Banaras Hindu University, Varanasi, India
[b] Department of Geophysics, Banaras Hindu University, Varanasi, India

ARTICLE INFO

Keywords:
CMIP6
Heat wave
Global climate model
Climate change
Extreme temperature

ABSTRACT

With rising global temperatures, extreme weather events have become more frequent, intense and of longer duration. CMIP6 GCMs provide improved climate simulations that need robust evaluation for historical period for reliable future projections. The present study assesses the ability of bias corrected CMIP6 14 Global Climate Models (GCMs) in simulating heat wave over India for March–June during the historical period (1951–2014). Heat waves were identified using IITM criteria. Model biases were removed using variance scaling bias correction method that showed higher correlation (0.93) and lower root mean square error (2.15) and improvement in approximating the inter-annual variability as well as spatial patterns as observed maximum temperature after bias correction. Evaluation of model performance for 95th and 99th percentile maximum temperature and heatwaves showed that most of the models simulate these extremes similar to observation. Northwestern, Central and South-central regions recorded highest number of heatwaves with a frequency of 50 heatwave days/decade, which were captured by the most of the GCMs varying in decadal frequency over the region. Among the GCM, although all models were found competent, ACCESS-ESM1–5, MPI-ESM1–2HR and MRI-ESM2–0 models were found to be the best performing models for extreme indices and heat wave simulation over India. The study will aid to the current understanding of CMIP6-GCMs performances over the different meteorological subdivisions of India and pave way for future projection of heat waves as well as reduction in uncertainty among the models.

1. Introduction

Extreme weather events in the wake of changing patterns of climate have emerged as a serious hazard around the globe and particularly over South-Asia region, causing huge loss of life as well as economic impacts (Chaudhury et al., 2000; Campbell et al., 2018; Mall et al., 2019, Hambrecht et al., 2022). The Intergovernmental Panel on Climate Change (IPCC) reports have stated that these events are likely to increase manifold in the future by the end of 21st century (Stocker et al., 2013; IPCC, 2021;). South Asian region has been witnessing rise in temperature which may cause rapid risk escalation in future, resulting in irreversible consequences,

* Corresponding author at: DST-Mahamana Centre of Excellence in Climate Change Research, Institute of Environment and Sustainable Development, Banaras Hindu University, Varanasi, India.
E-mail address: rkmall@bhu.ac.in (R.K. Mall).

https://doi.org/10.1016/j.uclim.2024.101936
Received 13 April 2023; Received in revised form 31 December 2023; Accepted 15 April 2024
Available online 30 April 2024

development issues, increased susceptibility to climatic hazards, conflict, and inequity (IPCC, 2021; Diffenbaugh and Giorgi, 2012; Mani et al., 2018). As per studies, in recent decades global region of heatwave hotspots are on the rise and there is an increase in the probability of occurrence of very extreme and extreme heatwave episodes by the end of 21st century (Russo et al., 2014). Compounding of heatwaves with drought and other extremes have increased the risk for the vulnerable population exacerbating its impact on the population (Baldwin et al., 2019). While Paris Agreement aims to limit the global warming to 1.5°-2 °C, it is still alarming as heatwave days are projected to increase by 4–34 days every season for every 1 °C rise which may be higher for regions (Perkins-Kirkpatrick and Gibson, 2017). Due to this unprecedented global warming climate extremes have shown a rise in frequency and severity over South-Asia and future projections shows a further rise in extremes including heat waves, flood and drought over the region making it as one of the global hotspots of climate change (Mukherjee et al., 2018; Aadhar and Mishra, 2020; Singh et al., 2021a, 2021b; Mall et al., 2022). There has been an unprecedented rise in the temperature extremes, which is likely to rise in future warming scenarios as well (Fischer et al., 2021; Saeed et al., 2021; Yaduvanshi et al., 2021; Singh and Mall, 2023; Singh et al., 2023). In addition to the high temperature the increase in minimum temperature have also been found to contribute to mortality in the South Asian region (Dimitrova et al., 2021; Mall et al., 2021). Perkins-Kirkpatrick and Gibson, 2017 proposed to develop a global unified network for better measurement and understanding of heatwaves and mechanisms behind it, as scientific literature lacks to define a complete mechanism of heatwaves. However, heat wave events have been found to be consistently strengthening crossing previous thresholds all over the world and impacting the global population as well as agriculture sector significantly (Knox et al., 2012; Lobell et al., 2012; Perkins, 2015; Singh and Mall, 2023).

India is among one of the most vulnerable countries to the rising extremes particularly heat waves observing numerous episodes of mortality in the recent decades and so heat wave events add to the morbidity and mortality burden of the country (Rohini et al., 2016; Singh et al., 2023; Singh et al., 2021a–d; Rajput et al., 2023; Singh et al., 2021a, 2021b). Pai et al. (2004) also observed increase in regional coverage, persistency and occurrences of heat-wave events during the period 1991–2000. The most populated and agriculture dominated region of India within the northern, central and northwestern parts have witnessed a multifold rise in heatwave frequency, duration and intensity in recent decades due to increase in maximum temperature (Dash and Hunt, 2007; Rohini et al., 2016; Panda et al., 2017; Singh et al., 2021a, 2021b). Among the most severe heat wave episodes over India, the year 1978–1999 observed huge mortality in the northern and eastern states of the country followed by many such episodes in the recent decades (De, 2000; Rohini et al., 2019). While heat wave events are increasing the efforts to model these extremes for generating accurate regional projections using regional and global climate models are also increasing. Simulation of extreme heat events using climate models have been one of focus research area of the climate scientists. Several studies have projected changes in heat wave events over India using both global and regional climate models which showed multifold rise in heat wave events in the future (Mishra et al., 2020; Rohini et al., 2019; Singh and Mall, 2023).

Among such efforts the Coupled Model Intercomparison project (CMIP) is an inter-model comparison project working primarily to improve model performances in simulating historical, present and future climate changes arising from natural changes under different emission scenarios based on radiative forcing scenarios in a multi-model framework. CMIP mainly focuses about the response of earth in different forcing scenarios, origins and consequences of systematic model biases and most importantly estimation of future climate changes for the variations in the forcing scenarios (Eyring et al., 2016). The modeling community strives to continuously improve the model simulations with each phase of the experiment and recent CMIP6 generation models are the most updated models that have the potential to offer new insights in the understanding of the global climate with better regional projections as well. In the CMIP6 phase different shared socioeconomic pathway (SSP) scenarios have been utilized for future extreme climate characterization, to understand the behavior of climate in different forcing scenario (Gusain et al., 2020; Schlund et al., 2020; Su et al., 2021). CMIP6, the most recent phase GCMs are being analyzed for their ability to simulate historical temperature variability and trends against observed global land surface temperature data indicating large variability in across model biases and regions (Fan et al., 2020; Almazroui et al., 2021; Zhao et al., 2023).

According to Fan et al., 2020, CMIP6 future projections indicate increased frequency and intensity of temperature extremes around the globe. CMIP6 experiment have also reported near permanent marine heatwaves occurrences around the globe (Plecha and Soares, 2020). The CMIP6 phase of the CMIP experiment provides the most recent climate projections with state-of-the-art climate models, which have been found satisfactory in various recent studies assessing extreme temperature events, extreme precipitation events in South Asia and Indian Summer Monsoon (ISM) simulations (Stouffer et al., 2017; Gusain et al., 2020; Seneviratne and Hauser, 2020; Hamed et al., 2022). An intercomparison study of CMIP5 and CMIP6 models over Korea shows that heatwaves and related teleconnection indices are better simulated by CMIP6 models than CMIP5 models (Kim et al., 2020). While model simulations may be perturbed by the associated bias, Mishra et al., 2020 showed that 13 biases corrected GCM output of CMIP6 experiment project 3° to 5 °C of warming along with 13–30% wetter climate by the end of 21st Century over South Asia. Several studies have been carried out using the CMIP6 GCMs for heat wave simulation over different cities and regions of India (Chatu et al., Das and Umamahesh, 2022; Dash et al., 2022; Nandi and Swain, 2022; Shukla and Attada, 2023). Kumar et al., 2022 analyzed heat wave events over four Indian cities. Das and Umamahesh, 2022 projected and compared heat wave occurrences over India using CMIP5 and CMIP6 GCMs for both representative concentration pathway (RCP) and SSP scenarios. The study found that heat wave is projected affect the presently unaffected regions of the country particularly, northeast, southern and western region and the magnitude projected under RCP scenarios are larger than the SSP scenarios. Though a comprehensive analysis, the study could have been more robust if there had been evaluation of heat wave simulations by the CMIP6 models for historical period for against the observation to account for uncertainty in projections. Dash et al., 2022 in a recent study over metropolitan cities of India using CMIP6 models found that frequency of warm nights and hot days the Chennai, Mumbai, Guwahati and Delhi (Dash et al., 2022). Nandi and Swain, 2022, evaluated the CMIP6 GCMs and analyzed future changes in heat wave characteristics over three South Indian Cities namely, Bangalore, Chennai and Hyderabad.

While the evaluation showed EC-Earth3-Veg model to best among 9 GCMs which shows that Chennai will be most affected by heat waves in future. Goyal et al., 2023 assessed the heat wave changes over the Indian smart cities and observed that the Coastal, Interior Peninsular, and North-Central regions with Thiruvananthapuram city observing most heat wave hazard in the future under SSP 245 and 585 scenarios. Shukla and Attada, 2023 examined the multi-model mean (MME) of 16 CMIP6 GCMs for the simulation of Universal Thermal Climate Index (UTCI) mean climatology for summer season over the northwest India (NWI) with ERA5 reanalysis data. The study found showed an increased thermal stress over NWI in the historical period which is captured by the MME and is projected to rise further at the rate of 0.09 °C per decade, 0.26 °C per decade, and 0.56 °C per decade in SSP1–2.6, SSP2–4.5, and SSP5–8.5 scenario rapidly raising a serious concern over the region. Rao et al., 2023 adopted a new approach of understanding the future risk associated with heat waves by using varying hazard thresholds such as fixed and decadal moving thresholds to declare heat wave and assess the future heat wave changes using CMIP6 models under different SSP scenarios over India. The findings reavealed that most of the models exhibit a higher mean temperature than the observed and further a significant increase in the heat wave in near future and far future using fixed thresholds as compared to the moving threshold which projected more increase in the far future period. However, Bhattacharya et al., 2023 found that CMIP6 models failed to approximate the spatial distribution of heat waves and cold waves over the over the climatic zones of India while investigating the trend and decadal variability in the frequency of heat waves and cold waves as compared to the observation. The above studies show that much emphasis is given to analyse the future changes in heat wave using CMIP6 models over isolated cities and climatic zones of India. However, comprehensive research evaluating the performance of CMIP6 experiments based heat wave events over the entire India region focusing on the meteorological subdivisions of the country. While future projections provide a set of possible sceanrios of heat wave hazard over the country, the reliability of these future projections

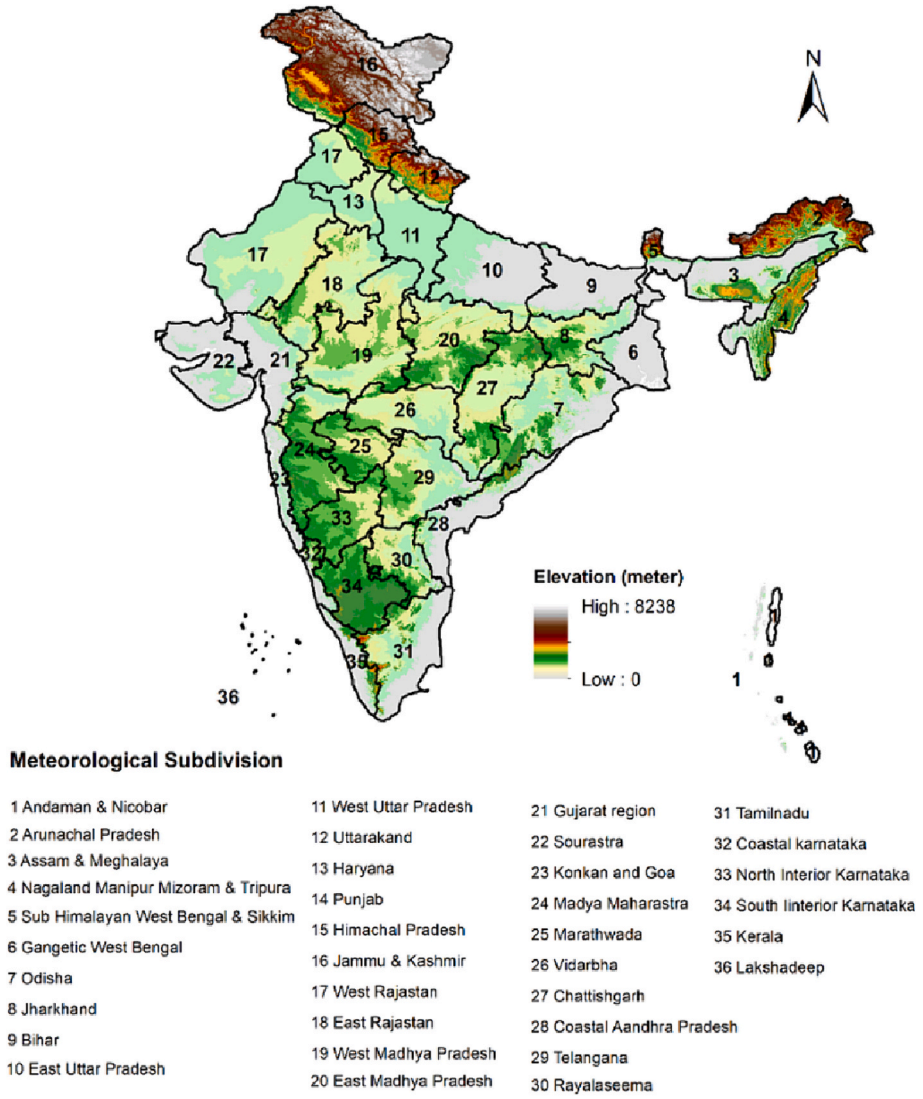

Fig. 1. India and its 36 meteorological subdivisions with topography.

require analysis of the ability of CMIP6 GCMs in simulating temperature extremes as well as heat wave events over the region. As the GCMs suffer from representing the sub-grid features accurately when compared to downscaled simulations it will be interesting to observe how the recent and most updated CMIP6 GCMs perform in representing the climatology over India.

The present study aims to evaluate the ability of CMIP6 GCMs in simulating daily gridded maximum temperature, climatological mean meaximum temperature, temperature extremes indices and frequency of heatwave events over the meteorological subdivisions of India for March–June during 1951–2014. The 14 CMIP6 model outputs which are available for the variable tasmax with consistent variant label r1i1p1f1 (for realization, initialization, physics and forcing) have been used for the in the study for studying the extreme temperature characteristics and simulation of heat wave over India and its meteorological subdivision. The study also intends to demonstrate the efficiency of bias corrected CMIP6 GCMs in simulating the seasonal maximum temperature climatology over India. For this investigation, maximum surface temperature variable of GCM outputs have been bias corrected using variance scaling approach to enhance model output against observed IMD data and validated as well. Further bias corrected data has been used to simulate extreme temperature indices and percentile-based threshold heat wave events over the country. This study will highlight the ability, deficiency and uncertainty associated with CMIP6 models in simulation of temperature extremes over different regions of India.

2. Data and methodology

2.1. Study area and data

The study is performed over India lying within the geographical extent of 8°4′N-37°0.6′ N latitude and 68°7′E-97°25′ E longitude. India covers a land area of 3.29 million square kilometers and is home to 1.35 billion people. The study has been carried out over the 36 meteorological subdivisions of India which are categorized based on homogeneity of the climate and differ in topography which influence the climate of the region (Attri and Tyagi, 2010) (Fig. 1).

India is one of the most heat wave affected region as March–June (MAMJ) months witness extreme heat over the subcontinent because of the development of pre-monsoon heat low. Around 3–7 heatwave spells are recorded every year during the MAMJ months (Rohini et al., 2019; Singh et al., 2021a, 2021b). Global climate models being coarser face challenges in the representation of the climate over such varied topography of the different subdivisions particularly in coastal and mountainous regions (Singh et al., 2021a, 2021b). The study intends to assess the model performance over the various meteorological subdivisions to find the best suitable model that performs cumulatively well for all of these subdivisions to account for the variation due to differing topography and climatological conditions. The study uses 14 GCMs from CMIP6 experiments archived at Earth System Grid Federation data node of World Climate Research Program (WCRP) (https://esgf-data.dkrz.de/search/esgf-dkrz/) for heat wave simulation analysis. The CMIP experiment stems from the need to improve the understanding of the past, present, and future climate change due to natural, unforced variability as well as radiative forcing changes in a multi-model environment. The CMIP6 phase of the CMIP experiment is the most updated generation of models and is a step ahead in terms of evolving from a single step central activity to a federal structure with 21 individual

Table 1
Details of CMIP6 GCMs used in the study.

Sr. no.	GCMS	Variant-id	Driving model Institution	Spatial Resolution	References
1.	ACCESS-ESM1–5	r1i1p1f1 & gn	Commonwealth scientific and industrial research organization/ Australia	1.25° × 1.25°	Bi et al. (2020)
2.	ACCESS-CM2			1.25° × 1.25°	Ziehn et al. (2020)
3.	AWI-CM-1-1-MR	r1i1p1f1 & gn	Alfred Wegener Institute Center for Environmental data analysis/ Germany	1.0° × 1.0°	Semmler et al. (2020)
4.	BCC-CSM2-MR	r1i1p1f1 & gn	Beijing Climate Center (BCC) China Meteorological Administration/China	1.125° × 1.125°	Wu et al. (2019)
5.	Can-ESM5	r1i1p1f1 & gn	Canadian Centre for Climate Modeling and Analysis/Canada	2.8° × 2.8°	Swart et al. (2019)
6.	CMCC-ESM2	r1i1p1f1 & gn	Euro-Mediterranean Centre on Climate Change coupled climate model/Italy	0.9° × 1.25°	Lovato et al. (2022)
7.	FGOALS-g3	r1i1p1f1 & gn	Chinese Academy of Sciences (CAS)/China	2.25° × 2.0°	Li et al., 2020
8.	MIROC6	r1i1p1f1 & gn	Model for Interdisciplinary Research on Climate (MIROC)/Japan	2.3272° × 1.1636°	Tatebe et al. (2019)
9.	MPI-ESM-1-2-LR	r1i1p1f1 & gn	Max Plank Institute for Meteorology/Germany	1.875° × 1.875°	Mauritsen et al. (2019)
10.	MPI-ESM-1-2-HR			0.9375° × 0.9375°	Müller et al. (2018)
11.	MRI-ESM2–0	r1i1p1f1 & gn	Meteorological Research Institute (MRI)/Japan	1.125° × 1.125°	Yaduvanshi et al. (2021)
12.	NorESM2-MM	r1i1p1f1 & gn	Norwegian Climate Centre/Norway	0.9375° × 1.25°	Seland et al. (2020)
13.	NorESM2-LM			1.875° × 2.5°	Seland et al. (2020)
14.	TaiESM1	r1i1p1f1 & gn	Taiwan Earth System Model/Taiwan	0.9° × 1.25°	Lee et al., 2020

model intercomparisons, a diagnostic experiment called DECK and historical simulations. The CMIP6 historical simulations are available from 1851 to 2014 and largely based on the observations. The simulations will assess the ability of models as compared to observation encompassing changes from natural forcings such as solar variability and volcanic aerosols and anthropogenic induced forcings such as CO2 concentration, aerosols, land use etc. (Eyring et al., 2016). Table 1 contains the details of the models used in the study for historical maximum temperature data on a daily frequency for the period 1951–2014 with common variant label r1i1p1f1, and native grid. Maximum temperature data was further extracted from the GCM data for the India region. Output of all the models were interpolated by performing nearest neighbor remapping to a homogenous $1.0^{\circ} \times 1.0^{\circ}$ spatial resolution. Daily gridded maximum temperature data at $1^{\circ} \times 1^{\circ}$ from India Meteorological department (IMD) for the period 1951–2014 (64 years) has been used as reference data. This gridded daily maximum temperature data was developed by using observations from 350 stations across India using Shephard's method (Srivastava et al., 2009). The heatwave assessment requires reliable maximum temperature data whereas the GCMs of CMIP6 experiment shows significant biases with respect to IMD data. So, meteorological variables from the output of GCMs must be bias corrected for reliable outcomes.

2.2. Variance scaling

Various bias correction methods are widely used to remove the biases in the climate data owing model systemic errors such as Variance Scaling, Mean Scaling, Quantile Mapping etc. Variance Scaling methods have been found to be significantly effective for removal of model biases for temperature variable (Teutschbein and Seibert, 2012; Bhatla et al., 2020; Singh et al., 2021a, 2021b). It scales the mean as well as the variance of the model output with respect to the observation and so after the model output is scaled the mean and variance of the bias corrected model data perfectly agrees with the reference data (IMD data for this study). Following the efficiency of the method the study utilizes variance scaling approach for bias correction of all 14 CMIP6 model output over India for the historical period (1951–2014).

Following steps are followed for variance scaling of historical model output:

(i) Difference of monthly mean values of model from observed is added to the model data

$$T1(d) = Tm(d) + \mu\,(To(d)) - \mu\,(Tm(d))$$

(ii) Deviations of model data from long term monthly mean are evaluated.

$$T2(d) = T1(d) - \mu\,(T1(d)).$$

(iii) Ratio of standard deviation of long term observed data to model data are multiplied by the result of Eq. (ii).

$$T3(d) = \frac{T2(d) \times [\sigma\,(To(d))]}{[\sigma\,(T2(d))]}$$

(iv) Long term monthly mean data are further added to Eq. (iii) to produce variance scaled model ouput.

$$Tmv(d) = T3(d) + \mu\,(Tm(d)).$$

The output of Eq. (iv) $Tmv(d)$, is the final bias corrected model output using variance scaling method. Here $To(d)$ and $Tm(d)$ are observed and model data respectively, whereas μ and σ are the operators for mean and standard deviation. For the validation of bias corrected model data, Taylor diagram constituting Correlation Coefficient (CC), Root Mean Square Deviation (RMSE) and Standard Deviations (SD) are calculated with IMD data as reference (Mann, 1945; Taylor, 2001; Gleckler et al., 2008). Probability distribution function and cumulative distribution functions are analyzed for the investigation of distribution pattern.

2.3. Analysis of temperature extremes

To analyse the ability of the model temperature extremes over India, 95th and 99th percentile values representing the extreme 5% and 1% of the daily temperature data over the study period were estimated. To identify heatwave events by analyzing the positive departure of maximum temperature from its daily normal value IITM criteria has been used (Mandal et al., 2019; Singh et al., 2021a, 2021b). As India witnesses extreme temperatures during the pre-monsoon season, heatwaves are computed for the March–June (MAMJ) months for the study period. Method for identifying heatwave using IITM is described by following steps:

(i) Maximum temperature should be greater than 95th percentile value.
(ii) Departure from normal should be $>3.5\ ^{\circ}C$ if Tmax $>36\ ^{\circ}C$.
(iii) Heatwave is declared when Tmax $>44\ ^{\circ}C$.

Therefore, heatwave is noted if the maximum temperature of region exceeds the normal temperature by 3.5 °C. On the other hand, if maximum temperature surpasses 44 °C heatwave is declared regardless of the percentile value. Further, Mann Kendall trend test has been used to analyse trend in maximum temperature as well as heat wave over India (Singh et al., 2021a, 2021b).

3. Results and discussion

The findings of the study can be explained into two parts, where the first objective is to improve the CMIP6 model outputs by removing the biases present in the data using variance scaling method. Whereas the second objective focuses on analyzing the extreme temperature indices and heatwave events over India for the period 1951–2014 using the bias corrected model data. The analysis of heatwaves over India using CMIP6 GCM data requires bias correction to make the model outputs more robust. In this study the variance scaling bias correction approach has been employed, which improves the variance of the model outputs by matching it with variance of the observed data. For the analysis, bias corrected model data has been further evaluated against the observed data for the period 1951–2014.

3.1. Evaluation of model performance

Fig. 2 shows the Probability Distribution Function (PDF) of historical maximum bias-corrected and raw/uncorrected CMIP6 model output for the period 1951 to 2014 (MAMJ) against the observed. Prior to bias correction, the results of the CMIP6 model exhibited higher standard deviations and lower mean maximum temperatures as compared to observed. The probability distribution shows that the models exhibit both cold and warm bias as the lower tail of the distribution lies below −20 °C and the upper tail reaches above 50 °C. However, the distribution shows that models underestimate the daily maximum temperature as the majority of models approximate the peak with a maximum probability at a surface temperature of slightly below 30 °C, where the observed temperature peak is around 32 °C. Variance scaling approach corrects the distribution of model data based on the mean, which initially displayed higher standard deviations than the IMD. After removal of bias in the model data, the dispersion from the mean and the mean value of the majority of the models were both improved satisfactorily and so agreed with the IMD mean. Both the cold and warm bias is significantly reduced as both the tail of the distribution matches closely with the observation after bias correction showing the improvement in the daily maximum temperature distribution.

Moreover, Taylor diagram of bias-corrected daily mean surface maximum temperature data of 14 CMIP6 models showed the Pearson CC, normalized SD and RMSE of different models with respect to IMD observed data over India (Fig. 3). The IMD baseline daily mean surface maximum temperature is represented by a red circle dot on the x-axis, whilst the CMIP6 raw and bias corrected daily mean surface maximum temperature data are represented by different geometric dots in the graphical space. The maximum surface temperature data from the IMD and model outputs are used to calculate the CC, SD, and RMSE for the historical period. Very significant standard deviations from IMD data, ranging from 8 to 12, have been observed in the raw model results (Table 2). Although, Correlation Coefficient values have been found significant ranging from 0.73 to 0.87 but the Root Mean Square Deviations have been found high, showing the dispersion of data (Table 3).

After bias correction, the CC between model outputs and IMD data improved significantly and the RMSE and SD values also improve, assuring that the output is consistent with the observed data. The multi-model mean shows best agreement with the observation. TaiESM1 was found to have highest correlation of 0.93, lowest RMSE of 2.15 and standard deviation of 5.16 after bias correction while NorESM2-MM showed relatively lower CC (0.86), higher RMSE (2.99) and SD (5.78). However, all of the CMIP6 model outputs showed similar results of the metric with minor variations (Table 2).

Followed by Taylor diagram, the yearly mean of temperature simulated by the models was further compared with the observations.

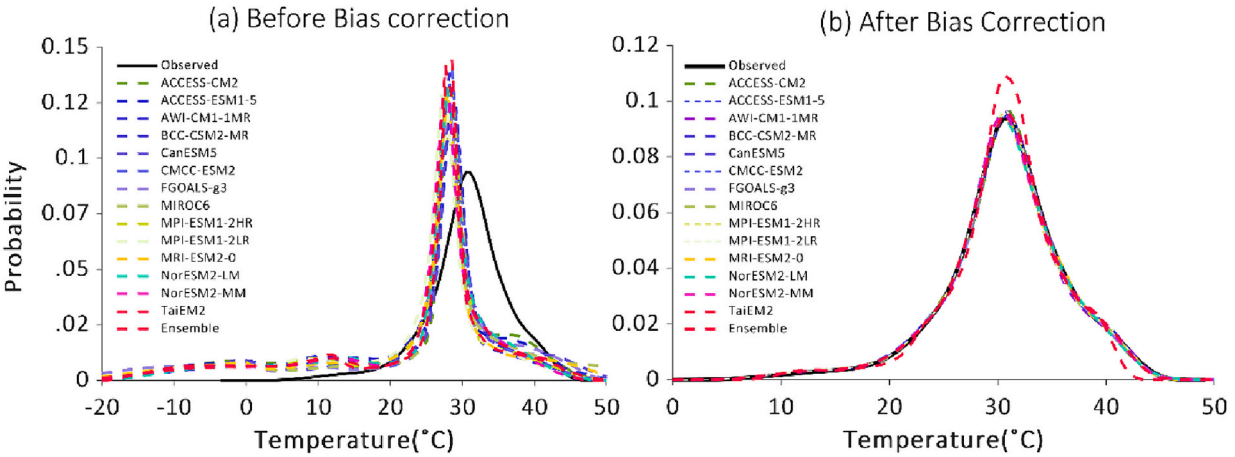

Fig. 2. Probability distribution function of maximum temperature data of CMIP6 models.

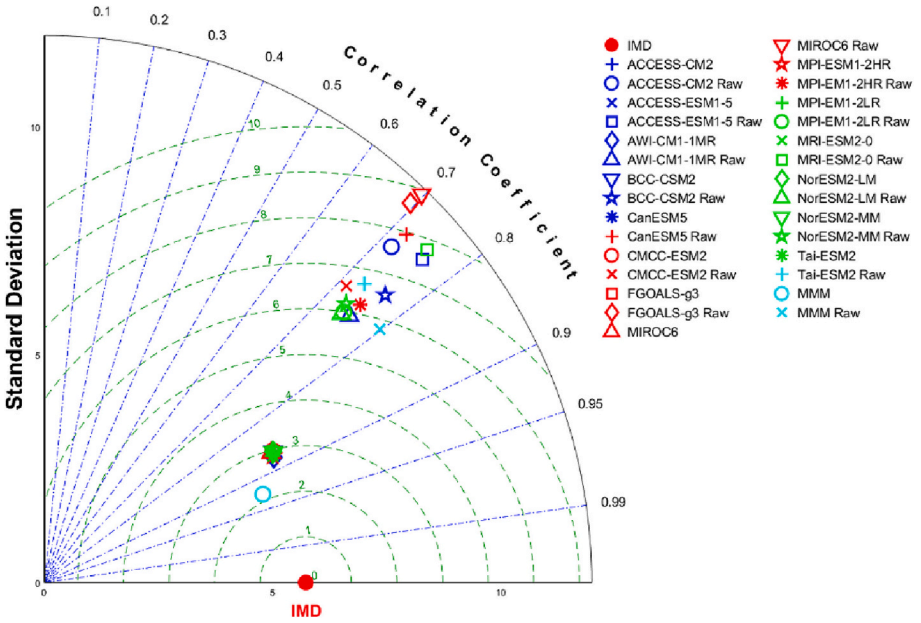

Fig. 3. Taylor diagram of Tmax variable for 14 CMIP6 models with IMD as reference data.

Table 2
Standard deviation, Correlation coefficient, and root mean square error of raw and bias corrected CMIP6 model output.

Models	Correlation Coefficient		Root Mean Square Error		Standard Deviation	
	Raw	Bias Corrected	Raw	Bias Corrected	Raw	Bias Corrected
ACCESS-CM2	0.72	0.87	7.60	2.91	10.59	5.72
ACCESS-ESM1–5	0.76	0.88	7.53	2.86	10.90	5.72
AWI-CM1–1MR	0.75	0.88	5.92	2.83	8.88	5.72
BCC-CSM2-MR	0.76	0.87	6.54	2.96	9.78	5.78
Can-ESM5	0.72	0.87	7.95	2.98	11.01	5.77
CMCC-ESM2	0.71	0.87	6.57	2.97	9.28	5.78
FGOALS-g3	0.70	0.87	8.89	2.95	11.87	5.73
MIROC6	0.75	0.87	6.21	2.87	9.22	5.73
MPI-ESM1–2HR	0.74	0.87	5.99	2.87	8.84	5.73
MPIESM1–2LR	0.75	0.87	7.77	2.87	11.13	5.73
MRI-ESM2–0	0.74	0.87	5.94	2.96	8.78	5.78
NorESM2-LM	0.73	0.87	6.17	2.94	9.00	5.78
NorESM2-MM	0.73	0.86	6.68	2.99	9.60	5.78
TaiESM1	0.80	0.93	5.78	2.15	9.21	5.16
MULTI- MODEL MEAN	0.69	0.87	8.63	2.97	11.56	5.78

It was found that all of the models underestimated the yearly mean for the historical period (1951–2014) for India, simulating within the range of 23 °C -27 °C whereas the observed yearly mean simulated around 30 °C (Fig. 4). The multi-model mean output showed highest variation against the observation. However, variance scaling was found to have improved the model simulated yearly mean. The coherency of the bias corrected data is more vigorous in ACCESS-ESM1–5, AWI-ESM1–1MR, MPI-ESM-HR and MIROC6 models with the observation.

Quantiles and mean of maximum temperature data distribution of all models show lower values as compared to IMD data. Uncorrected model outputs possess lesser variability as compared to the observed maximum temperature. For observed maximum temperature, the 25th and 75th quantiles are 28 °C and 32 °C, respectively, which is higher than the corresponding quantiles for all the model-simulated values. First and third quantiles for bias corrected models were reported approximately 26 °C and 33 °C, respectively. Nevertheless, a few outliers were also found in ACCESS-CM2, BCC-CSM2-MR, and NorESM2-LM. As compared to the uncorrected model data, where all model medians were much below 30 °C, the median for bias corrected models were improved to 30 °C as of IMD data. Since, the variance scaling based bias correction method improves scales the model outputs on both mean and standard deviation metric with respect to the observation so after bias correction the maximum temperature distribution with mean, median and quantiles matches well with the observation and have been shown by several studies related to extreme temperature and rainfall events (Teutschbein and Seibert, 2012; Bhatla et al. 2020; Singh et al., 2021a, 2021b). It is due to this reason that the box plots of bias corrected maximum temperature data shows improvements in mean distribution with respect to IMD data as shown in Fig. 5b.

Table 3
Heatwave events (1951–2014) over various meteorological subdivisions of India.

Meteorological Sub division	Observed	Multi-Model Mean	Range
Gangetic West Bengal	211	175	113–237
Odisha	126	153	111–190
Jharkhand	260	203	168–275
Bihar	241	164	104–216
East Uttar Pradesh	335	262	210–374
West Uttar Pradesh	396	324	280–444
Haryana Chandigarh & Delhi	367	334	303–400
Punjab	282	252	230–298
Rajasthan West	338	331	320–368
Rajasthan East	350	325	341–379
East Madhya Pradesh	276	267	292–313
West Madhya Pradesh	321	279	228–397
Gujarat	166	163	112–220
Marathwada	113	147	82–230
Vidarbha	289	307	215–386
Chhattisgarh	210	194	119–264
Coastal Andhra Pradesh	125	136	84–203
Telangana	184	213	153–270

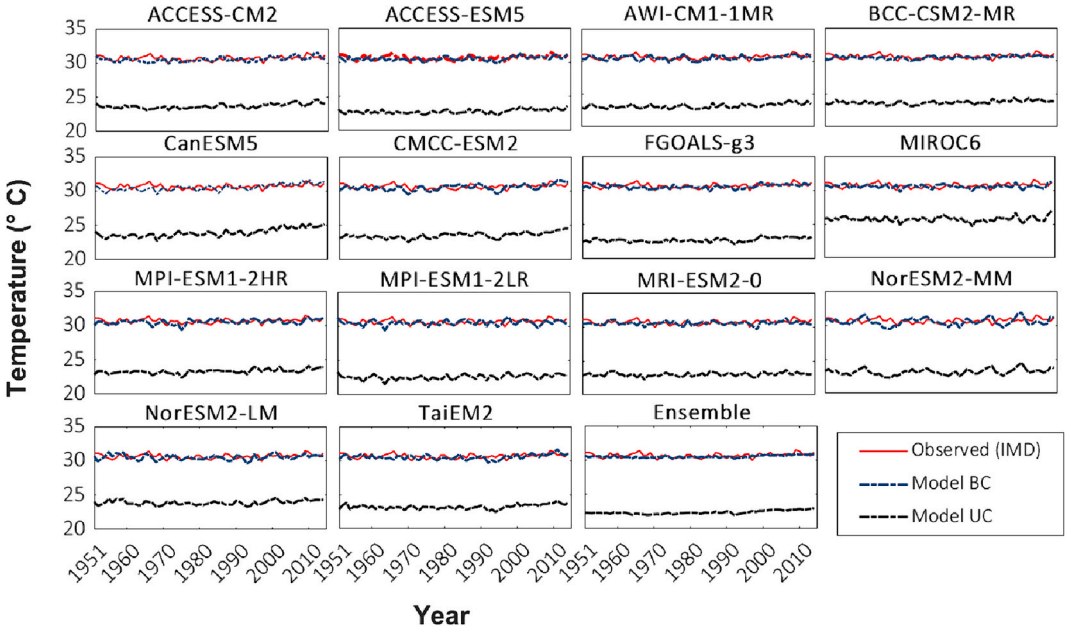

Fig. 4. Variation of yearly mean maximum temperature 14 CMIP6 model output against the observation for 1951–2014.

However, variability of maximum temperature is improved for most of the models after bias correction except ACCESS-CM2 and MPI-ESM1–2HR show higher variability and deviation (Fig. 6). Also, there is a marginally declining trend of maximum temperature over the West Bengal and Uttarakhand states of India with a rate of about 0.005 °C per year. The rising surface maximum temperature trend over peninsular India is simulated by ACCESS-ESM1–5, AWI-CM1–1MR, CMCC-ESM2, MPI-ESM1–2HR, and MRI-ESM2–0 models similar to the observations. However, the rising trend over Northeast India is well replicated by ACCESS-CM2, AWI-CM1–1MR, CanESM5, and MPI-ESM1–2LR in agreement with observation. However, while CanESM5 is showing an overestimation in the temperature trend over all of the subdivisions, NorESM-LM and NorESM-MM show an underestimation over most of the subdivisions making them inferior to other models of the experiment.

The declining trend over eastern region is over estimated by ACCESS-CM2, MIROC6, and NorESM2-MM, but ACCESS-ESM1–5, MPI-ESM1–2HR, MPI-ESM1–2LR and MRI-ESM2–0 perform best over this region. While the observed temperature trends are in agreement with the observations reported by Ross et al., 2018 and Rao et al., 2023, similar trends were observed for ACCESS-CM2, ACCESS-ESM1–5, MPI-ESM1–2LR and MRI-ESM2–0. simulated maximum temperature by Rao et al., 2023. Multi-Model mean of all models shows similar trend as of observed with a slightly lower rate over most of the regions except the Jammu & Kashmir/ Ladakh region. However, the CMIP6 models were found to be underestimating the overall magnitude of maximum temperature trend over India. Similar observations regarding CMIP6 models were made by Hamed et al., 2022 when compared with the IMD observations.

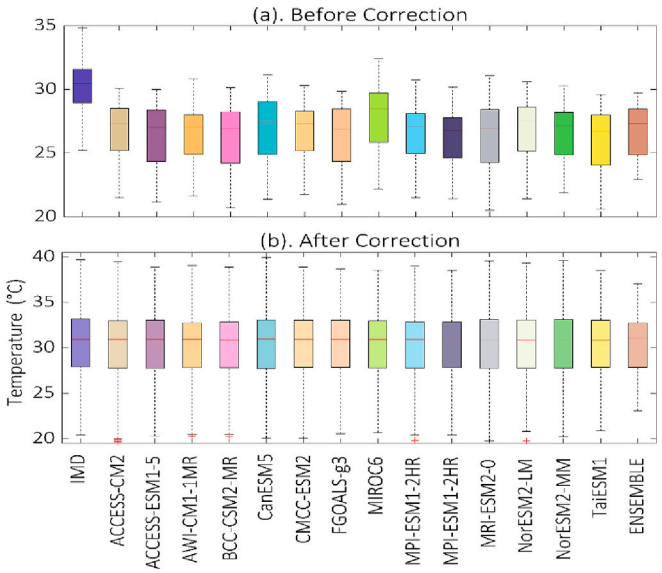

Fig. 5. Boxplot showing maximum temperature distribution of CMIP6 model output (a) before bias correction and (b) after bias correction.

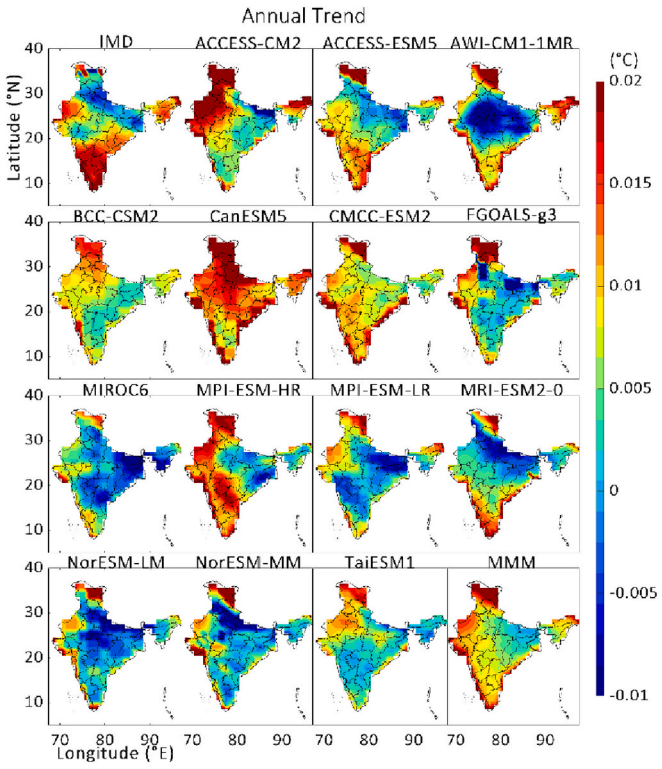

Fig. 6. Spatial trend of daily maximum surface temperature data for the period 1951–2014.

3.2. Extreme temperature analysis and evaluation of heatwaves

For the evaluation of the model ability for simulating extreme temperature over India long term 3 day running 95th and 99th percentiles have been calculated for March–April-May-June (MAMJ) months of the whole study period (Fig. 7). Extreme temperature values are different for different subdivision of India owing to different geographical features. The highest 95th and 99th percentile values using the IMD data have been observed over the central and western regions with values ranging between 42 °C to 44 °C. These

regions have been reported to observe higher temperature along with northwestern India by several studies due to consistent rising temperature trends in the regions in these recent decades (Ross et al., 2018; Rohini et al., 2019; Goyal et al., 2023). These regions occasionally witness temperature as high as 50 °C during the pre-monsoon period due to the development of heat low of summer monsoon. The northern states of Himanchal and Uttarakhand show lower 95th and 99th percentile values ranging from 30 °C to 35 °C due to higher altitude. However, these regions historically have not been prone to heatwave events (Pai et al., 2013; Mandal et al., 2019; Singh et al., 2021a, 2021b).

Simulations of the bias corrected CMIP6 models show good results as all 14 models depict the 95th percentile maximum temperature similar to the reference IMD data for all the subdivision(Fig. 7a). However, models namely ACCESS-CM2, ACCESS-ESM1–5, FGOALS-g3 show higher 95th percentile values than IMD over the western Uttar Pradesh and Northern Madhya Pradesh region. Similarly, the 99th percentile values representing the extreme threshold have also been simulated by the CMIP6 models which also agree with the observation IMD (Fig. 7b). Over the Central, Northern, and Western regions higher maximum surface temperatures for the 99th percentile have been very well estimated. The multi-model mean percentiles were found to be closest to the observed data.

Heatwave events were calculated using the IITM criteria which utilizes long term 3 day running 95th percentile temperature values to evaluate extreme temperature events (Fig. 8a). Heatwave days in this method are declared on the basis if the temperature exceeds 95th percentile of daily temperature for each grid where the daily temperature must be higher than 36 °C and departure from mean should be >3.5 °C, also heatwave is declared if temperature exceeds 44 °C irrespective of probability of exceedance (Mandal et al., 2019). Observed data shows most frequent heatwave events over the western Uttar Pradesh, Madhya Pradesh, northern parts of Rajasthan and Delhi ranging between a total of 500 to 550 days for the MAMJ season of the study period (1951–2014). However, Central, Northern, Northwestern and Central eastern regions witness around 300 heatwave days during the 64 years of the study period. Eastern Maharashtra, Chhattisgarh, and Telangana region have also been found to be heatwave prone with >300 heatwave events. Shukla and Attada, 2023 while analyzing the thermal discomfort over the Indian region also found that the northwestern and central cities are prone to higher thermal discomfort as compared to other cities of the country. While the spatial distribution of heat wave occurrence may be similar to the observations, models differ in simulating the magnitude or frequency of heat wave days over India. ACCESS-CM2, CanESM5, and NorESM2-MM overestimates the number of heatwaves over Northwestern region constituting of East and West Rajasthan meteorological subdivisions. MPI-ESM, NorESM2, and FGOALs-g3 have been found to simulate approximately equal number of heatwave days over similar regions. The increasing and decreasing trend by the observation and CMIP6 models are also reported by recent studies by Rao et al., 2023; Goyal et al., 2023.

Decadal average of heatwave events has been calculated to measure the decadal frequency of extreme temperatures over various regions (Fig. 8b). With an average of >50 heatwave occurrences every decade, western Uttar Pradesh and parts of northwestern Madhya Pradesh followed by the northwestern and northern regions with 30 days/decade, these regions have been identified to be as the most frequently observed heatwave regions. Similar results have been reported by Singh et al., 2021a and Singh et al., 2021b. Also, it is interesting to note that the eastern Maharashtra region also observes >30 heatwave occurrences over a decade. New heatwave hotspots have been developing over the peninsular India in the recent decades (Singh et al., 2021a, 2021b). The multi-model mean and range of estimated mean of total heatwave events over various Indian meteorological subdivisions of India for MAMJ during 1951–2014 have been estimated (Table 3). The results show that the number of heat wave days over meteorological subdivisions within the eastern and central-eastern region i.e., West Rajasthan (331) and East Rajasthan (325), West Uttar Pradesh (324), East Uttar Pradesh (262), West Madhya Pradesh (279), East Madhya Pradesh (267), Telangana (213), Vidarbha (307), Chhattisgarh (194) Jharkhand (203), Odisha (153), were highest. Higher number of heat waves in the coastal region of the country pose a severe health risk to the inhabitants (Singh et al., 2021a, 2021b). As the model simulations over the regions showing similar occurrence of heat waves indicates towards the added value in the latest CMIP6 models which despite being global climate models are able to capture the topography and coastal characteristics intrinsic to the regions. 6 of the 14 CMIP6 model simulations i.e., AWI-CM1–1MR, CanESM5, FGOALS-g3, MPI-ESM1–2HR, NorESM2-LM and NorESM2-MM replicates the observed relatively well in the heatwave frequency whereas the ACCESS-ESM1–5 underestimates and ACCESS-CM2 model overestimates the most.

3.3. Trend analysis

Mann-Kendall trend test at 5% significance level was applied to evaluate the heatwaves trend simulated by the models against observed over India and different subdivisions for MAMJ (1951–2014). According to the observed trend, heatwave frequency has increased over northwestern, central, central-eastern regions of India (Fig. 8). However, the eastern region including Gangetic West Bengal, Bihar, Jharkhand subdivisions with an overall decreasing trend. Singh et al., 2021a, 2021b., found similar results for the region in both frequency and trend where the seasonal average heat wave events were higher in the Gangetic West Bengal due to higher frequency in the early decades of 1950s, 1960s which decreased gradually in the recent decades causing a declining trend. Similar trends have been observed in the decrease of maximum temperature but the rate of HW frequency decrease is higher over West Bengal region compared to Uttarakhand (Fig. 8). ACCESS-CM2 and CanESM5 models overestimated the trend over the northwestern, central and south-central region showing significantly increasing trend over these regions whereas the rising trend in the northwestern parts were reasonably simulated by ACCESS-ESM1–5, MPI-ESM1–2HR, MPI-ESM1–2LR, NorESM2-MM and TaiESM1. While the decreasing trend over the Gangetic West Bengal was found to be simulated by the MIROC6, MPI-ESM1–2HR, MPI-ESM1–2LR and MRI-ESM2–0, it was also observed that these models simulated negative trends over most of the regions of the country. TaiESM1 and the multi-model mean simulated the heat wave days similar to the observation in both spatial distribution and temporal frequency as well as the declining trend in the eastern region. Overall, the trend analysis found that ACCESS-ESM1–5, TaiESM1 and the multi-model were best among all the 14 CMIP6 models for India and can be used reliably for future projections.

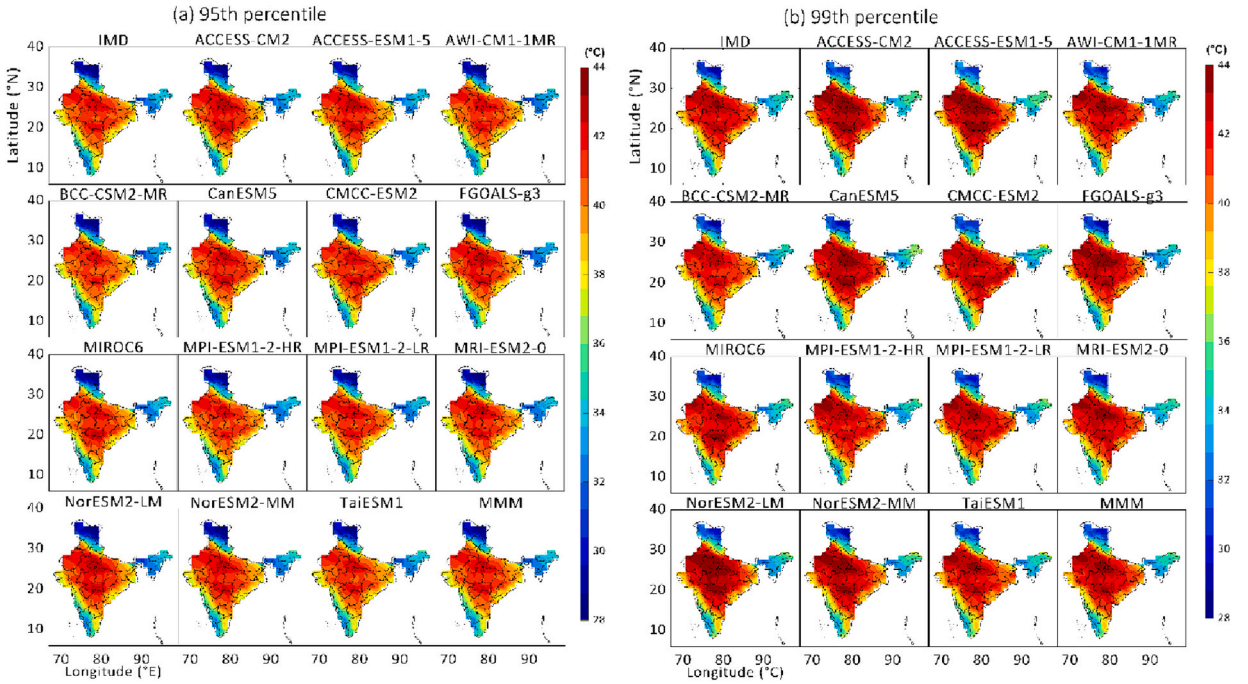

Fig. 7. Spatial distribution of extreme temperature distribution by CMIP6 bias corrected model output for the period 1951–2014 (a) 95th percentile (b) 99th Percentile.

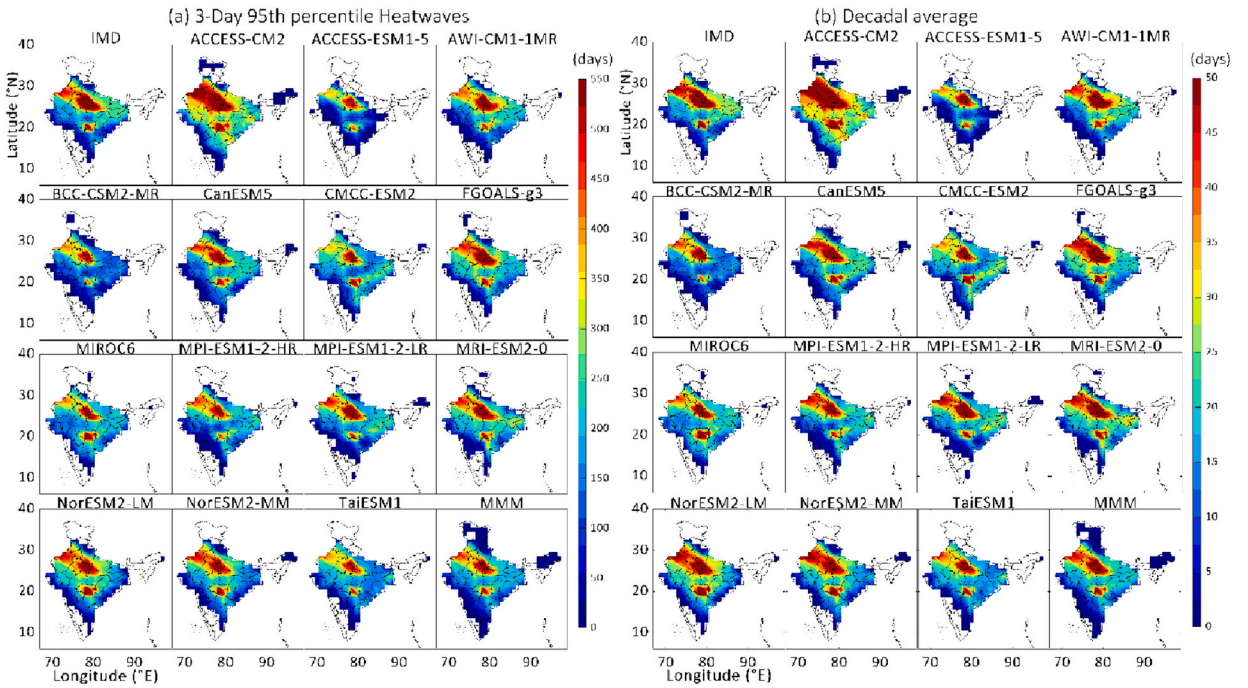

Fig. 8. Heatwave events over India calculated by IITM criteria. (a). Cumulative heatwave events during the period 1951–2014. (b) Decadal average of Heatwave events.

4. Conclusion

India has become a hotspot for heat wave rise and its severe impact on human health, agriculture and economy. The present study assessing the recent CMIP6 model performance for heat wave simulation over India found that the bias corrected CMIP6 GCMs show consistency in the simulation of temperature and extremes temperature over India and its subdivision. Although, annual variations of bias corrected model results show improvement, but performances of different models are found better in different regions. ACCESS-ESM1–5, MPI-ESM1–2HR, and MRI-ESM2–0 have been found to be the best models in temperature simulations over different regions of India. Furthermore, extreme temperature analysis shows highest values of 95th and 99th percentiles over the Central, Northern and Central-western regions. Further, heat wave analysis revealed that the eastern and central and south-central meteorological subdivisions, e.g., Odisha, Jharkhand, Gangetic west Bengal, Bihar, Telangana, Vidarbha and Chhattisgarh recorded highest number of heatwave events. There is an increase in heatwave trend over northwestern and central eastern parts of India and a decrease over the Gangetic west Bengal region. These trends were very well replicated by ACCESS-ESM1–5, MPI-ESM1–2HR, MPI-ESM1–2LR, MRI-ESM2–0, NorESM2-MM and TaiESM1. This study concludes that bias corrected CMIP6 models are efficient in simulating the maximum temperature, extreme temperature and heatwave events over India. Although, all models were found competent, ACCESS-ESM1–5, MPI-ESM1–2HR and MRI-ESM2–0 models were best out of 14 CMIP6 models. As the CMIP6 models pave way for improved understanding and simulation of extreme temperature events for the future modeling studies, the present study will help to better understand the performance of CMIP6 based model outputs in simulation of heat waves over India. The findings of the study will aid in ascertaining the uncertainties associated with uncorrected model performances and help in reducing in future experiments as well as making reliable future projections of extreme temperature and heat waves over India.

Funding information

Authors thank the Climate Change Programme, Department of Science and Technology, New Delhi for financial support (DST/CCP/CoE/ 80/2017(G)).

CRediT authorship contribution statement

Saumya Singh: Investigation, Validation, Visualization, Writing – original draft, Data curation, Methodology. **R.K. Mall:** Conceptualization, Funding acquisition, Methodology, Project administration, Resources, Supervision, Writing – review & editing. **Praveen K. Singh:** Formal analysis, Investigation, Software, Writing – original draft. **R. Bhatla:** Writing – review & editing. **Pawan K. Chaubey:** Data curation, Visualization.

Declaration of competing interest

The authors declare no conflict of interest.

Data availability

All of the CMIP6 Global Climate model data used in the study is available at https://esgf-data.dkrz.de/search/esgf-dkrz/. The IMD data can be accessed on request from https://cdsp.imdpune.gov.in/. Authors declare that all data and materials support their published claims and comply with field standards.

Acknowledgments

Authors thank the Climate Change Programme, Department of Science and Technology, New Delhi, for financial support (DST/CCP/CoE/80/2017(G)). Authors gratefully acknowledge the climate modeling groups contributing to CMIP6 project and making their model output available (listed in Table 1). The authors thank the Earth System Grid Federation (ESGF) infrastructure and India Meteorological Department, New Delhi for providing the meteorological data.

References

Aadhar, S., Mishra, V., 2020. Increased drought risk in South Asia under warming climate: implications of uncertainty in potential evapotranspiration estimates. J. Hydrometeorol. 21 (12), 2979–2996. https://doi.org/10.1175/JHM-D-19-0224.1.

Almazroui, M., Saeed, F., Saeed, S., Ismail, M., Azhar, M., 2021. Projected changes in climate extremes using CMIP6 simulations over SREX regions. Earth Syst. Environ. 5 (3), 481–497. https://doi.org/10.1007/s41748-021-00250-5.

Attri, S.D., Tyagi, A., 2010. Climate profile of India. Environ. Meteorol. India Meteorol. Dep. 1–122 https://doi.org/10.1007/s12524-010-0015-9.

Baldwin, J.W., Dessy, J.B., Vecchi, G.A., Oppenheimer, M., 2019. Temporally compound heat wave events and global warming: An emerging hazard. Earth's Fut. 7 (4), 411–427. https://doi.org/10.1029/2018EF000989.

Bhatla, R., Sarkar, D., Verma, S., Sinha, P., Ghosh, S., Mall, R.K., 2020. Regional climate model performance and application of bias corrections in simulating summer monsoon maximum temperature for agro-climatic zones in India. Theor. Appl. Climatol. 142, 1595–1612. https://doi.org/10.1007/s00704-020-03393-z.

Bhattacharya, A., Thomas, A., Soni, V.K., Roy, P.S., Sarangi, C., Kanawade, V.P., 2023. Opposite trends in heat waves and cold waves over India. J. Earth Syst. Sci. 132 (2) https://doi.org/10.1007/s12040-023-02069-2.

Bi, D., Dix, M., Marsland, S., O'farrell, S., Sullivan, A., Bodman, R., Law, R., Harman, I., Srbinovsky, J., Rashid, H.A., Dobrohotoff, P., 2020. Configuration and spin-up of ACCESS-CM2, the new generation Australian community climate and earth system simulator coupled model. J. Southern Hemisph. Earth Syst. Sci. 70 (1), 225–251. https://doi.org/10.1071/ES19040.

Campbell, S., Remenyi, T.A., White, C.J., Johnston, F.H., 2018. Heatwave and health impact research: A global review. Health Place 53, 210–218. https://doi.org/10.1016/j.healthplace.2018.08.017.

Chaudhury, S.K., Gore, J.M., Ray, K.S., 2000. Impact of heat waves over India. Curr. Sci. 79 (2), 153–155.

Das, J., Umamahesh, N.V., 2022. Heat wave magnitude over India under changing climate: projections from CMIP5 and CMIP6 experiments. Int. J. Climatol. 42 (1), 331–351. https://doi.org/10.1002/joc.7246.

Dash, S.K., Hunt, J.C.R., 2007. Variability of climate change in India. Curr. Sci. 782–788.

Dash, S.K., Saraswat, V., Panda, S.K., Pattnayak, K.C., 2022. Temperature extremes and their future projections in selected Indian cities along with their meteorological subdivisions and temperature homogeneous zones. Urban Clim. 41, 101057 https://doi.org/10.1016/j.uclim.2021.101057.

De, U.S., 2000. Weather and climate related impacts on health in megacities. WMO Bull. 49, 340–348. https://doi.org/10.3389/frsc.2021.705131.

Diffenbaugh, N.S., Giorgi, F., 2012. Climate change hotspots in the CMIP5 global climate model ensemble. Clim. Chang. 114, 813–822. https://doi.org/10.1007/s10584-012-0570-x.

Dimitrova, A., Ingole, V., Basagana, X., Ranzani, O., Mila, C., Ballester, J., Tonne, C., 2021. Association between ambient temperature and heat waves with mortality in South Asia: systematic review and meta-analysis. Env. Int. 146, 106170 https://doi.org/10.1016/j.envint.2020.106170.

Eyring, V., Bony, S., Meehl, G.A., Senior, C.A., Stevens, B., Stouffer, R.J., Taylor, K.E., 2016. Overview of the coupled model Intercomparison project phase 6 (CMIP6) experimental design and organization. Geosci. Model Dev. 9, 1937–1958. https://doi.org/10.5194/gmd-9-1937-2016.

Fan, X., Duan, Q., Shen, C., Wu, Y., Xing, C., 2020. Global surface air temperatures in CMIP6: historical performance and future changes. Environ. Res. Lett. 15 (10), 104056 https://doi.org/10.1088/1748-9326/abb051.

Fischer, E.M., Sippel, S., Knutti, R., 2021. Increasing probability of record-shattering climate extremes. Nat. Clim. Chang. 11 (8), 689–695. https://doi.org/10.1038/s41558-021-01092-9.

Gleckler, P.J., Taylor, K.E., Doutriaux, C., 2008. Performance metrics for climate models. J. Geophys. Res. Atmos. 113 (D6), 1–20. https://doi.org/10.1029/2007JD008972.

Goyal, M.K., Singh, S., Jain, V., 2023. Heat waves characteristics intensification across Indian smart cities. Sci. Rep. 1–16 https://doi.org/10.1038/s41598-023-41968-8.

Gusain, A., Ghosh, S., Karmakar, S., 2020. Added value of CMIP6 over CMIP5 models in simulating Indian summer monsoon rainfall. Atmos. Res. 232, 104680 https://doi.org/10.1016/j.atmosres.2019.104680.

Hambrecht, E., Tolhurst, R., Whittaker, L., 2022. Climate change and health in informal settlements: a narrative review of the health impacts of extreme weather events. Environ. Urban. 34 (1), 122–150. https://doi.org/10.1177/09562478221083896.

Hamed, M.M., Nashwan, M.S., Shahid, S., Bin Ismail, T., Wang, X.J., Dewan, A., Asaduzzaman, M., 2022. Inconsistency in historical simulations and future projections of temperature and rainfall: A comparison of CMIP5 and CMIP6 models over Southeast Asia. Atmos. Res. 265, 105927 https://doi.org/10.1016/j.atmosres.2021.105927.

IPCC, 2021. Summary for policymakers. In: Masson-Delmotte, V., Zhai, P., Pirani, A., Connors, S.L., Péan, C., Berger, S.N., et al. (Eds.), Climate Change 2021: The Physical Science Basis. Contribution of Working group I to the Sixth Assessment report of the intergovernmental panel on climate change. Cambridge University Press, Cambridge, United Kingdom and New York, NY, USA, pp. 3–32. https://doi.org/10.1017/9781009157896.001.

Kim, M.K., Yu, D.G., Oh, J.S., Byun, Y.H., Boo, K.O., Chung, I.U., et al., 2020. Performance evaluation of CMIP5 and CMIP6 models on heatwaves in Korea and associated teleconnection patterns. J. Geophys. Res. Atmos. 125 (23) https://doi.org/10.1029/2020JD032583 e2020JD032583.

Knox, J., Hess, T., Daccache, A., Wheeler, T., 2012. Climate change impacts on crop productivity in Africa and South Asia. Environ. Res. Lett. 7 (3), 034032 https://doi.org/10.1088/1748-9326/7/3/034032.

Kumar, P., Rai, A., Upadhyaya, A., Chakraborty, A., 2022. Analysis of heat stress and heat wave in the four metropolitan cities of India in recent period. Sci. Total Environ. 818, 151788. https://doi.org/10.1016/j.scitotenv.2021.151788.

Lee, W.-L., Wang, Y.-C., Shiu, C.-J., Tsai, I., Tu, C.-Y., Lan, Y.-Y., Chen, J.-P., Pan, H.-L., Hsu, H.-H., 2020. Taiwan earth system model version 1: description and evaluation of mean state. Geosci. Model Dev. 13, 3887–3904. https://doi.org/10.5194/gmd-13-3887-2020.

Li, L., Yu, Y., Tang, Y., Lin, P., Xie, J., Song, M., Dong, L., Zhou, T., Liu, L., Wang, L., Pu, Y., 2020. The flexible global ocean-atmosphere-land system model grid-point version 3 (FGOALS-g3): description and evaluation. J. Adv. Model. Earth Syst. 12 (9) e2019MS002012.

Lobell, D.B., Sibley, A., Ivan Ortiz-Monasterio, J., 2012. Extreme heat effects on wheat senescence in India. Nat. Clim. Chang. 2 (3), 186–189.

Lovato, T., Peano, D., Butenschön, M., Materia, S., Iovino, D., Scoccimarro, E., Fogli, P.G., Cherchi, A., Bellucci, A., Gualdi, S., Masina, S., 2022. CMIP6 simulations with the CMCC earth system model (CMCC-ESM2). J. Adv. Model. Earth Syst. 14 (3) https://doi.org/10.1029/2021MS002814 p.e2021MS002814.

Mall, R.K., Srivastava, R.K., Banerjee, T., Mishra, O.P., Bhatt, D., Sonkar, G., 2019. Disaster risk reduction including climate change adaptation over South Asia: challenges and ways forward. Int. J. Disaster Risk Sci. 10 (1), 14–27. https://doi.org/10.1007/s13753-018-0210-9.

Mall, R.K., Chaturvedi, M., Singh, N., Bhatla, R., Singh, R.S., Gupta, A., Niyogi, D., 2021. Evidence of asymmetric change in diurnal temperature range in recent decades over different agro-climatic zones of India. Int. J. Climatol. 1–14. https://doi.org/10.1002/joc.6978.

Mall, R.K., Singh, N., Patel, S., Singh, S., Arora, A., Bhatla, R., et al., 2022. Climate changes over the Indian subcontinent: Scenarios and impacts. In: Khare, N. (Ed.), Science, Policies and Conflicts of Climate Change. Springer Climate. Springer, Cham. https://doi.org/10.1007/978-3-031-16254-1_2.

Mandal, R., Joseph, S., Sahai, A.K., Phani, R., Dey, A., Chattopadhyay, R., Pattanaik, D.R., 2019. Real time extended range prediction of heat waves over India. Sci. Rep. 9 (1), 1–11. https://doi.org/10.1038/s41598-019-45430-6.

Mani, M., Bandyopadhyay, S., Chonabayashi, S., Markandya, A., 2018. South Asia's hotspots: The impact of temperature and precipitation changes on living standards. In: South Asia Development Matters. World Bank, Washington, DC. Accessed from. https://openknowledge.worldbank.org/handle/10986/28723.

Mann, H.B., 1945. Nonparametric tests against trend. Econometrica 245–259.

Mauritsen, T., Bader, J., Becker, T., Behrens, J., Bittner, M., Brokopf, R., Brovkin, V., Claussen, M., Crueger, T., Esch, M., Fast, I., 2019. Developments in the MPI-M earth system model version 1.2 (MPI-ESM1. 2) and its response to increasing CO2. J. Adv. Model. Earth Syst. 11 (4), 998–1038. https://doi.org/10.1029/2018MS001400.

Mishra, V., Bhatia, U., Tiwari, A.D., 2020. Bias-corrected climate projections for South Asia from coupled model intercomparison project-6. Sci. data 7 (1), 1–13. https://doi.org/10.1038/s41597-020-00681-1.

Mukherjee, S., Aadhar, S., Stone, D., Mishra, V., 2018. Increase in extreme precipitation events under anthropogenic warming in India. Weath. Climat. Extrem. 20, 45–53. https://doi.org/10.1016/j.wace.2018.03.005.

Müller, W.A., Jungclaus, J.H., Mauritsen, T., Baehr, J., Bittner, M., Budich, R., et al., 2018. A higher-resolution version of the max planck institute earth system model (MPI-ESM1. 2-HR). J. Adv. Model. Earth Syst. 10 (7), 1383–1413. https://doi.org/10.1029/2017MS001217.

Nandi, S., Swain, S., 2022. Analysis of heatwave characteristics under climate change over three highly populated cities of South India: a CMIP6-based assessment. Environ. Sci. Pollut. Res. 1–13. https://doi.org/10.3390/su141911892.

Pai, D.S., Thapliyal, V., Kokate, P.D., 2004. Decadal variation in the heat and cold waves over India during 1971-2000. Mausam 55 (2), 281–292. https://doi.org/10.54302/mausam.v55i2.1083.

Pai, D.S., Nair, S., Ramanathan, A.N., 2013. Long term climatology and trends of heat waves over India during the recent 50 years (1961-2010). Mausam 64 (4), 585–604. https://doi.org/10.54302/mausam.v64i4.742.

Panda, D.K., AghaKouchak, A., Ambast, S.K., 2017. Increasing heat waves and warm spells in India, observed from a multiaspect framework. J. Geophys. Res. Atmos. 122 (7), 3837–3858. https://doi.org/10.1002/2016JD026292.

Perkins, S.E., 2015. A review on the scientific understanding of heatwaves—their measurement, driving mechanisms, and changes at the global scale. Atmos. Res. 164, 242–267. https://doi.org/10.1016/j.atmosres.2015.05.014, 2015 Oct 1.

Perkins-Kirkpatrick, S.E., Gibson, P.B., 2017. Changes in regional heatwave characteristics as a function of increasing global temperature. Sci. Rep. 7 (1), 1–12. https://doi.org/10.1038/s41598-018-23085-z.
Plecha, S.M., Soares, P.M., 2020. Global marine heatwave events using the new CMIP6 multi-model ensemble: from shortcomings in present climate to future projections. Environ. Res. Lett. 15 (12), 124058 https://doi.org/10.1088/1748-9326/abc847.
Rajput, P., Singh, S., Singh, T.B., Mall, R.K., 2023. The nexus between climate change and public health: a global overview with perspectives for Indian cities. Arab. J. Geosci. 16 (1), 15. https://doi.org/10.1007/s12517-022-11099-x.
Rao, K.K., Jyoteeshkumar Reddy, P., Chowdary, J.S., 2023. Indian heatwaves in a future climate with varying hazard thresholds. Environ. Res.: Clim. 2 (1), 015002 https://doi.org/10.1088/2752-5295/acb077.
Rohini, P., Rajeevan, M., Srivastava, A.K., 2016. On the variability and increasing trends of heat waves over India. Sci. Rep. 6 (1), 1–9. https://doi.org/10.1038/srep26153.s.
Rohini, P., Rajeevan, M., Mukhopadhay, P., 2019. Future projections of heat waves over India from CMIP5 models. Clim. Dyn. 53 (1), 975–988. https://doi.org/10.1007/s00382-019-04700-9.
Ross, R.S., Krishnamurti, T.N., Pattnaik, S., Pai, D.S., 2018. Decadal surface temperature trends in India based on a new high-resolution data set. Sci. Rep. 8 (1), 1–10. https://doi.org/10.1038/s41598-018-25347-2.
Russo, S., Dosio, A., Graversen, R.G., Sillmann, J., Carrao, H., Dunbar, M.B., Singleton, A., Montagna, P., Barbola, P., Vogt, J.V., 2014. Magnitude of extreme heat waves in present climate and their projection in a warming world. J. Geophys. Res. Atmos. 119 (22), 12–500.
Saeed, F., Schleussner, C.F., Ashfaq, M., 2021. Deadly heat stress to become commonplace across South Asia already at 1.5 C of global warming. Geophys. Res. Lett. 48 (7) https://doi.org/10.1002/2014JD022098 p.e2020GL091191.
Schlund, M., Lauer, A., Gentine, P., Sherwood, S.C., Eyring, V., 2020. Emergent constraints on equilibrium climate sensitivity in CMIP5: do they hold for CMIP6? Earth Syst. Dynam. *11* (4), 1233–1258. https://doi.org/10.5194/esd-11-1233-2020.
Seland, Ø., Bentsen, M., Olivié, D., Toniazzo, T., Gjermundsen, A., Graff, L.S., Debernard, J.B., Gupta, A.K., He, Y.C., Kirkevåg, A., Schwinger, J., 2020. Overview of the Norwegian earth system model (NorESM2) and key climate response of CMIP6 DECK, historical, and scenario simulations. Geosci. Model Dev. 13 (12), 6165–6200. https://doi.org/10.5194/gmd-13-6165-2020.
Semmler, T., Danilov, S., Gierz, P., Goessling, H.F., Hegewald, J., Hinrichs, C., Koldunov, N., Khosravi, N., Mu, L., Rackow, T., Sein, D.V., 2020. Simulations for CMIP6 with the AWI climate model AWI-CM-1-1. J. Adv. Model. Earth Syst. 12 (9) https://doi.org/10.1029/2019MS002009 p.e2019MS002009.
Seneviratne, S.I., Hauser, M., 2020. Regional climate sensitivity of climate extremes in CMIP6 versus CMIP5 multimodel ensembles. Earth's Future 8 (9). https://doi.org/10.1029/2019EF001474 p.e2019EF001474.
Shukla, K.K., Attada, R., 2023. CMIP6 models informed summer human thermal discomfort conditions in Indian regional hotspot. Sci. Rep. 1–14 https://doi.org/10.1038/s41598-023-38602-y.
Singh, N., Chaturvedi, M., Mall, R.K., 2023. Unraveling diurnal asymmetry of surface temperature under warming scenarios in diverse agroclimate zones of India. Theor. Appl. Climatol. 152, 321–335. https://doi.org/10.1007/s00704-023-04407-2.
Singh, S., Mall, R.K., 2023. Frequency dominates intensity of future heat waves over India. Iscience 26 (11). https://doi.org/10.1016/j.isci.2023.108263.
Singh, N., Mall, R.K., Banerjee, T., Gupta, A., 2021d. Association between climate and infectious diseases among children in Varanasi city, India: A prospective cohort study. Sci. Total Environ. 796, 148769. https://doi.org/10.1016/j.scitotenv.2021.148769.
Singh, S., Mall, R.K., Dadich, J., Verma, S., Singh, J.V., Gupta, A., 2021a. Evaluation of CORDEX- South Asia regional climate models for heat wave simulations over India. Atmos. Res. 248, 105228 https://doi.org/10.1016/j.atmosres.2020.105228.
Singh, S., Mall, R.K., Singh, N., 2021b. Changing spatio-temporal trends of heat wave and severe heat wave events over India: an emerging health hazard. Int. J. Climatol. 41, E1831–E1845. https://doi.org/10.1002/joc.6814.
Singh, N., Mhawish, A., Banerjee, T, Ghosh, S, Singh, RS, Mall, RK., 2021c. Association of aerosols, trace gases and black carbon with mortality in an urban pollution hotspot over central Indo-Gangetic Plain. Atmos. Environ. 246, 118088. https://doi.org/10.1016/j.atmosenv.2020.118088.
Srivastava, A.K., Rajeevan, M., Kshirsagar, S.R., 2009. Development of a high resolution daily gridded temperature data set (1969–2005) for the Indian region. Atmos. Sci. Lett. 10 (4) https://doi.org/10.1002/as pp.249-254. 254.
Stocker, T.F., Qin, D., Plattner, G.K., Alexander, L.V., Allen, S.K., Bindoff, N.L., Bréon, F.M., Church, J.A., Cubasch, U., Emori, S., Forster, P., 2013. Technical summary. In: Climate Change 2013: The Physical Science Basis. Contribution of Working Group I to the Fifth Assessment Report of the Intergovernmental Panel on Climate Change. Cambridge University Press, pp. 33–115.
Stouffer, R.J., Eyring, V., Meehl, G.A., Bony, S., Senior, C., Stevens, B., Taylor, K.E., 2017. CMIP5 scientific gaps and recommendations for CMIP6. Bull. Am. Meteorol. Soc. 98 (1), 95–105. https://doi.org/10.1175/BAMS-D-15-00013.1.
Su, B., Huang, J., Mondal, S.K., Zhai, J., Wang, Y., Wen, S., et al., 2021. Insight from CMIP6 SSP-RCP scenarios for future drought characteristics in China. Atmos. Res. 250, 105375 https://doi.org/10.1016/j.atmosres.2020.105375.
Swart, N.C., Cole, J.N., Kharin, V.V., Lazare, M., Scinocca, J.F., Gillett, N.P., et al., 2019. The Canadian earth system model version 5 (CanESM5. 0.3). Geosci. Model Dev. 12 (11), 4823–4873. https://doi.org/10.5194/gmd-12-4823-2019.
Tatebe, H., Ogura, T., Nitta, T., Komuro, Y., Ogochi, K., Takemura, T., et al., 2019. Description and basic evaluation of simulated mean state, internal variability, and climate sensitivity in MIROC6. Geosci. Model Dev. 12 (7), 2727–2765. https://doi.org/10.5194/gmd-12-2727-2019.
Taylor, K.E., 2001. Summarizing multiple aspects of model performance in a single diagram. J. Geophys. Res. Atmos. 106 (D7), 7183–7192. https://doi.org/10.1029/2000JD900719.
Teutschbein, C., Seibert, J., 2012. Bias correction of regional climate model simulations for hydrological climate-change impact studies: review and evaluation of different methods. J. Hydrol. 456 https://doi.org/10.1016/j.jhydrol.2012.05.052 pp.12-29. 12–29.
Wu, T., Lu, Y., Fang, Y., Xin, X., Li, L., Li, W., Jie, W., Zhang, J., Liu, Y., Zhang, L., Zhang, F., 2019. The Beijing climate center climate system model (BCC-CSM): the main progress from CMIP5 to CMIP6. Geosci. Model Dev. 12 (4), 1573–1600. https://doi.org/10.5194/gmd-12-1573-2019.
Yaduvanshi, A., Nkemelang, T., Bendapudi, R., New, M., 2021. Temperature and rainfall extremes change under current and future global warming levels across Indian climate zones. Weath. Clim. Extrem. 31, 100291 https://doi.org/10.1016/j.wace.2020.100291.
Zhao, Y., Cheruy, F., Thiery, W., 2023. Heatwave characteristics in the recent climate and at different global warming levels : A multimodel analysis at the global scale earth ' s. Future 1–18. https://doi.org/10.1029/2022EF003301.
Ziehn, T., Chamberlain, M.A., Law, R.M., Lenton, A., Bodman, R.W., Dix, M., Stevens, L., Wang, Y.P., Srbinovsky, J., 2020. The Australian earth system model: ACCESS-ESM1. 5. J. Southern Hemisphere Earth Syst. Sci. 70 (1), 193–214.